Available online at www.sciencedirect.com

ScienceDirect

Green Energy & Environment 1 (2016) 4–17

www.keaipublishing.com/gee

Review article

# Recent progress in rechargeable alkali metal–air batteries

Xin Zhang, Xin-Gai Wang, Zhaojun Xie*, Zhen Zhou**

*Tianjin Key Laboratory of Metal and Molecule Based Material Chemistry, Institute of New Energy Material Chemistry, Collaborative Innovation Center of Chemical Science and Engineering (Tianjin), School of Materials Science and Engineering, National Institute for Advanced Materials, Nankai University, Tianjin 300350, China*

Received 16 February 2016; revised 11 March 2016; accepted 14 March 2016
Available online 12 April 2016

**Abstract**

Rechargeable alkali metal–air batteries are considered as the most promising candidate for the power source of electric vehicles (EVs) due to their high energy density. However, the practical application of metal–air batteries is still challenging. In the past decade, many strategies have been purposed and explored, which promoted the development of metal–air batteries. The reaction mechanisms have been gradually clarified and catalysts have been rationally designed for air cathodes. In this review, we summarize the recent development of alkali metal–air batteries from four parts: metal anodes, electrolytes, air cathodes and reactant gases, wherein we highlight the important achievement in this filed. Finally problems and prospective are discussed towards the future development of alkali metal–air batteries.


*Keywords:* Metal–air batteries; Alkali metal anodes; Electrolytes; Ionic liquids; Air cathodes

## 1. Introduction

Fast economic development and huge energy consumption have spawned rapid decrease of fossil fuels along with large emission of $CO_2$. To sustain the non-renewable resources and reduce $CO_2$ emission, the only way out is to develop new energy. The great harvest of recent investigations on new energy is inspiring, and will accelerate the transformation of fossil fuel based economy to clean energy economy [1–3]. Batteries, whose capacity to efficiently convert and store electrical energy was recognized early on, have been used in a myriad of applications extending from portable electronic devices and grid-scale energy storage to electric vehicles (EVs) [4–6]. Among all kinds of batteries so far, lithium-ion batteries have captured the market due to high gravimetric and volumetric capacity as well as good energy efficiency [1].

Nowadays, it is a global trend to develop EVs – starting from hybrid EVs to plug-in EVs and ultimately to pure EVs – which use state-of-the-art lithium-ion batteries for propulsion, as a measure to reduce the gasoline consumption and mitigate $CO_2$ emission [7]. However, due to the high cost and insufficient energy density of current EV batteries, EVs account for a small fraction of the car market. Currently, EVs powered with lithium-ion batteries have a driving range limited to 160 km upon a single charge [8]. Tremendous research efforts have been dedicated to increase the energy density of lithium-ion batteries. However, the energy density of lithium-ion batteries is around 100–200 Wh $kg^{-1}$, which cannot achieve the long term goal in term of EVs [9]. Therefore, novel energy storage systems with higher energy density are extremely desired.

On the road of searching for energy storage systems with higher energy density, metal–air batteries have received great interest. According to the available research, several metal–air

* Corresponding author.
** Corresponding author.
*E-mail addresses:* zjxie@nankai.edu.cn (Z. Xie), zhouzhen@nankai.edu.cn (Z. Zhou).

http://dx.doi.org/10.1016/j.gee.2016.04.004

batteries have been proposed and studied, such as lithium–air, sodium–air, zinc–air, magnesium–air, aluminum–air, and potassium–air batteries. All the above batteries have very high theoretical energy density about 2–10 folds higher than that of lithium-ion batteries [10]. That makes them promising candidates for next-generation driving power of EVs. Table 1 summarizes the voltage, theoretical specific capacity and energy density of different metal–air batteries. The theoretical specific capacity is based on the total mass of the anode and cathode, including $O_2$ ($\varepsilon_M = -nFE/\Sigma M$, where F is the Faraday constant, E is the electrochemical reaction potential and M is the molecular weight of reactants). Among all the metal–air batteries, Li–air, Na–air, K–air and Zn–air batteries are regarded as rechargeable ones. Although a few studies of rechargeable Al–air and Mg–air batteries have been reported recently [11,12], their cyclic ability is very limited; therefore, these metal–air batteries are not included in this review.

Metal–air batteries are roughly comprised of four parts: metal anode, electrolyte, separator and air cathode (Fig. 1). The separator is an insulator which can only allow the transformation of ions. In the discharge process, oxidation reactions occur to the metal anode with metal dissolved in the electrolyte and oxygen reduction reaction (ORR) is induced in the air cathode. Due to the open battery configuration that uses air as the reactant, metal–air batteries own much higher specific capacity. Although they have high energy density, there are tremendous challenges in these systems that must be overcome before they are put into practical uses.

In this review, we focus on the recent progress of alkali metal–air batteries: Li–air, Na–air and K–air batteries. This review is divided into four parts: metal anodes, electrolytes, air cathodes and reactant gases. In each section, we will separately discuss recent progress of alkali metal–air batteries.

## 2. Metal anodes

In most alkali metal–air batteries, alkali metal plates are used as anodes. They possess much benefit including high reversibility, low equivalent weight and high specific capacity. As we know, alkali metals are very active. They can react with electrolytes at the surface, and form a passivation layer known as solid electrolyte interphase (SEI) film covering the alkali metal. Currently, the study of SEI film is mainly on Li-ion batteries and Li-metal secondary batteries [13–16]. The results show that SEI film sharply influences the performance of

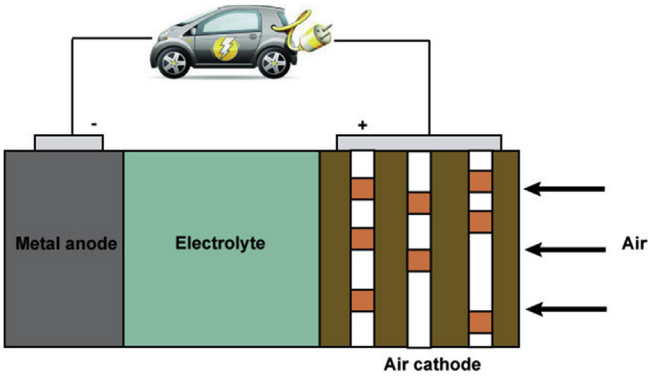


Fig. 1. Schematic configuration of metal–air batteries.

batteries and plays an important role in determining the deposition morphology.

The first study of SEI film in the presence of $O_2$ was conducted by Younesi et al. [17]. They investigated the composition and stability of SEI film forming in Li–$O_2$ batteries and identified various chemical species. The composition of SEI film is affected by the presence of oxygen, and is unstable during cycling. The SEI film mainly contains esters, LiF, carboxylates and alkoxides. Compared with non-air batteries, Li–$O_2$ batteries showed higher amount of C and O, while the relative amount of Li and F is lower. It was also found that the composition of SEI changed with the different stages of batteries. The concentration of carbonates decreases during the discharge process while increases during charge. The electrolyte used in their study was 1 M $LiPF_6$ in propylene carbonate (PC). This electrolyte cannot form stable SEI film to maintain the stability of Li metals. When the electrolyte of $LiClO_4$ in PC was used, a stable SEI layer formed. Li–$O_2$ batteries, with metallic Li pretreated with this electrolyte as the anode, exhibited enhanced cyclic ability [18]. Younesi et al. indicated that the SEI film with the electrolyte of $LiClO_4$ in PC was mainly made of polyethylene oxide (PEO), carboxylates, carbonates and $LiClO_4$ [19]. Walker et al. pointed out the important role of stable SEI film in Li–$O_2$ batteries [20]. They found that the electrolytes of 0.5 M lithium bis(-trifluoromethane sulfonimide) (LiTFSI) in *N*,*N*-dimethylacetamide (DMA) cannot form stable SEI film on the Li anode although DMA is regarded as an outstanding solvent for air batteries. Replacing LiTFSI with $LiNO_3$, a protective SEI film formed on Li due to the existence of nitrate anions. The reduction of nitrate anions on Li metal occurred according to

Table 1
Parameters and reactions of various metal–air batteries.

| Batteries | Voltage (V) | Theoretical specific capacity (Ah/kg) | Theoretical energy density (Wh $kg^{-1}$) | Reaction |
|---|---|---|---|---|
| Al–air | 2.71 | 1030 | 2791 | $4Al + 3O_2 + 6H_2O \rightarrow 4Al(OH)_3$ |
| Mg–air | 3.09 | 920 | 2843 | $Mg + 1/2O_2 + H_2O \rightarrow Mg(OH)_2$ |
| Zn–air | 1.65 | 658 | 1085 | $Zn+1/2O_2 \leftrightarrow ZnO$ |
| Li–air | 2.96 | 1170 | 3463 | $2Li + O_2 \leftrightarrow Li_2O_2$ |
| Na–air | 2.27 | 487 | 1105 | $Na + O_2 \leftrightarrow NaO_2$ |
| | 2.33 | 687 | 1600 | $2Na + O_2 \leftrightarrow Na_2O_2$ |
| K–air | 2.48 | 377 | 935 | $K + O_2 \leftrightarrow KO_2$ |

the reaction, $2Li + LiNO_3 \rightarrow Li_2O + LiNO_2$. The stable SEI film inhibits reactions between the solvent and Li anode. $LiNO_3$ is also a good electrolyte additive to improve the stability of SEI film. Lee et al. used X-ray photoelectron spectroscopy (XPS) and Fourier Transform infrared spectroscopy (FTIR) to measure chemical aspect of oxygen dissolved in a dimethyl sulfoxide (DMSO)-based electrolyte on lithium metal. They found that the SEI film contains $Li_3N$, $Li_2S_2O_4$, $Li_2S$, $LiCF_3$, and $Li_2O$, which is unstable [21]. To improve the stability of SEI, $LiNO_3$ was added to DMSO [22].

Besides SEI films, dendrites are another factor drastically affecting the performance of metal-based batteries. Dendrites form during the discharge and charge processes, caused by the uncontrollable dissolution and deposition of metal anodes, since metals do not necessarily deposit onto the site where it was consumed. Dendrites gradually generated during the cycles. Dendrites can penetrate the membrane and cause an internal short circuit with cathodes, degrading the performance of batteries, or even worse, causing explosions. This problem has long puzzled researchers. It seems difficult to control the deposition of metals by an orderly way. Although there is no report that Li/K dendrites penetrate the separator in Li/K–$O_2$ batteries, Hartmann et al. observed that Na dendrites penetrate the pores of the polymer separator after 10 cycles, and they proposed that the growth of sodium dendrites is the reason for the limited capacity retention of Na–air batteries [23]. The dendrite in metal–air batteries seriously influences their performances. By summarizing the experience from the development of Li-metal batteries, one can see that replacing Li metal with an anode material of Li-ion batteries is a simple way to solve the dendrite issue. This effective strategy can also be used in other alkali metal–air batteries. Sun et al. used a lithiated silicon-carbon composite as the anode of Li–air batteries, the safety hazard associated with the use of the highly reactive Li metal can be addressed [24]. They also reported a nanostructured lithiated tin–carbon composite as an alternative anode. Dispersing tin nanoparticles in a micrometric carbon matrix resulted in the formation of stable SEI film and avoided the undesired side reactions originating from the oxygen crossover [25]. Also, a lithiated Al–carbon composite electrode was prepared through an electrochemical method and was then applied to Li–$O_2$ batteries. Compared with Li–$O_2$ batteries with metallic Li anodes, Li–$O_2$ batteries with $Li_xAl$–C anodes displayed better cycling performance [26].

Sodium metal could likewise be replaced by sodiated carbon based on a carbon gas diffusion layer in sodium–air batteries, as reported by Bender and coworkers [27]. It increased the cycle life by a factor of 5 and further decreased the sum of the charge and discharge overpotentials due to the improved stability of the metal anode. The authors pointed out that the current limitation of Na–air batteries are mainly caused by the metal anode rather than the air cathode.

The larger ionic radius of potassium causes significant restrictions on the use of intercalation-type electrodes due to layer exfoliation upon intercalation [28]. An alloying strategy may be used instead. William et al. reported that K–Sb alloys can be used as the anode of potassium–air batteries [28]. The batteries exhibited a reversible capacity of 650 mAh $g^{-1}$ (98% of the theoretical capacity, 660 mAh $g^{-1}$) corresponding to the formation of a cubic $K_3Sb$ alloy.

Although the above approaches might solve the problem of metal dendrites and improve the stability, they would limit the specific energy of the batteries. By contrast, making an artificial film on the metal surface is an alternative way, since it can both control the flow of metal ions and ensure uniform metal deposition. Cui group proposed an innovative method to coat lithium with a monolayer of interconnected amorphous hollow carbon nanospheres, and it helped isolate the lithium metal deposition and facilitated the formation of stable SEI film. The coulombic efficiency improved to ~99% for over 150 cycles [29]. Lee and coworkers reported a composite protective layer comprising $Al_2O_3$ and polyvinylidene fluoride-hexafluoro propylene for Li metal anodes, which resulted in a dramatic enhancement of the cycling stability of Li–$O_2$ batteries [30]. $Al_2O_3$ can provide a mechanical strength sufficient to suppress dendrites. For this consideration, Kang et al. only used $Al_2O_3$ membrane with uniform, nanometer-sized pores as protected layer for Li metal anodes of Li–$O_2$ batteries [31]. Indeed, the uniform pores can provide pathways for ion transportation. The schematic illustration is shown in Fig. 2 for uniform, nanoscopic pores of $Al_2O_3$ membrane. Zhang et al. used an electrochemical strategy to obtain LiF-containing protection film on Li metal; the treated Li metal was used as anodes for Li–air batteries and significantly improved the cycling stability [32]. Compared with Li–$O_2$ batteries, Na–$O_2$ batteries have cleaner cathode reactions, but equally have low cycle life, which is perhaps caused mainly by the Na anode. Dendrites are the main reason for the failure of batteries. To prevent dendrite penetration, a sodium ion selective membrane was employed in the battery construction, and it improved the cycle life of Na–$O_2$ batteries from 12 cycles to 120 cycles [33].

The stability and safety of alkali metal anodes are common issues in alkali metal-based batteries, not only alkali metal–air batteries but also Li–S batteries which are regarded as next-generation batteries. Unfortunately, until now there have no satisfactory solutions yet, and more efforts are still necessary in this direction.

## 3. Electrolytes

The electrolyte is a critical part for such open systems of alkali metal–air batteries. It closely relates to the performance of batteries. Each metal–air system has its own demand for the characteristics of electrolytes. Overall, finding a stable, low volatility, non-toxic and high oxygen solubility electrolyte with a wide electrochemical window is a common goal for all systems. Numerous researchers hammer at studying the electrolyte for alkali metal–air batteries. Presently, there are several kinds of electrolytes that have widely been studied, including aqueous electrolytes, organic electrolytes, room temperature ionic liquids and solid-state electrolytes. We will

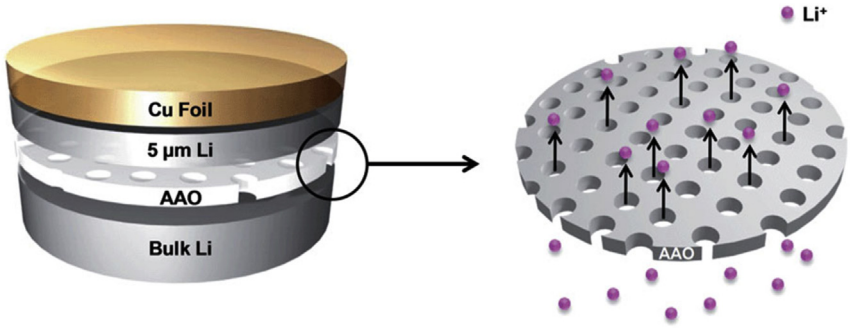


Fig. 2. Schematic illustration of uniform, nanoscopic pores of $Al_2O_3$ membrane [27].

discuss these four kinds of electrolytes separately, as well as liquid phase catalysts for metal–air batteries.

### 3.1. Aqueous electrolytes

Since alkali metals are too active to contact directly with aqueous electrolytes, researchers have to design batteries with a special construction, solid waterproof ion conduction layer to protect the metal from aqueous electrolytes. Currently, the most successful solid layer for alkali metal–air batteries is the commercial NASICON-type glass-ceramics. The popularity of this sort of solid layers is owing to its high ion conductivity and mechanical strength, as well as its chemical stability in water, mild acids and bases. However, because of the instability of many solid layers in contact with alkali metals, a "buffer" layer is needed between the alkali metal anode and the solid layer. There are two different battery constructions according to the type of buffer layers: "hybrid" and "aqueous", as shown in Fig. 3. Both batteries use aqueous electrolytes at the cathode side. Two kinds of half-cell reactions occur depending on the pH of aqueous electrolytes. The half-cell reactions are shown as follows:

$$O_2 + 2H_2O + 4e^- \leftrightarrow 4OH^- \quad E_0 = 0.4\ V\ (vs.\ RHE) \tag{1}$$

$$O_2 + 4H^+ + 4e^- \leftrightarrow 2H_2O \quad E_0 = 1.23\ V\ (vs.\ RHE) \tag{2}$$

For the alkaline catholyte (electrolyte on the cathode side), alkali hydroxide solutions are commonly used. Hashimoto and Hayashi used nanoporous gold (NPG) as the cathode for hybrid Na–air batteries, wherein a ceramic separator NASICON was applied as the solid layer [34]. The aqueous electrolyte is 1 M NaOH solution. They compared hybrid batteries with non-aqueous batteries which also used NPG as the cathode, and found that the hybrid batteries exhibited lower overpotential and better round-trip efficiency. According to their report, the large resistance of ORR in non-aqueous batteries was relieved by changing the catholyte into the aqueous electrolyte, which makes the hybrid batteries afford higher rate capability and power density [34]. In another study by Sun et al., the hybrid Na–air batteries which also used NASICON as the solid layer and NaOH solution as the catholyte showed good rechargeability, while Pt/C-coated carbon paper was used as air cathodes [35]. Similarly, LiOH solution was also used as the catholyte for Li–air batteries [36–40]. However, LiOH will be consumed during long-term charging, which in turn increases the internal resistance. To solve this problem, $LiNO_3$ and LiCl were added into the electrolyte to decrease the internal resistance [41]. As for the alkali catholyte, $CO_2$ ingression is a big problem. Therefore, acidic catholytes are needed. Up to date, the acidic catholyte was only reported in Li–air batteries. Li et al. reported hybrid Li–air batteries with sulfuric acid as the catholyte. The good performance of batteries indicated that sulfuric acid is a viable catholyte [42]. Nevertheless, due to the instability of solid layers in strong acids, it is not appropriate to make use of strong acids. Imidazole has a strong ability to absorb protons in water which

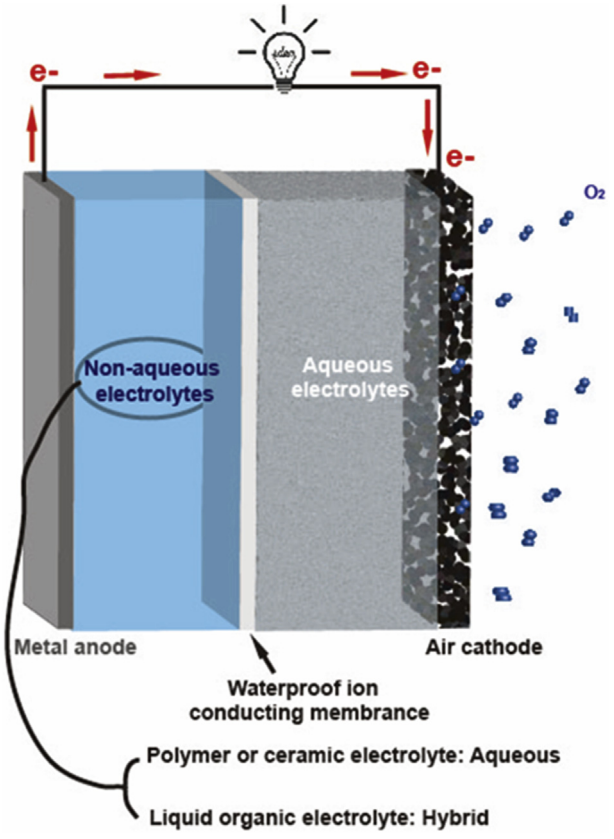


Fig. 3. Schematic configuration of hybrid and aqueous alkali metal–air batteries.

can act as a proton reservoir. Adding imidazole into strong acids can adjust the pH value of electrolytes and alleviate the corrosion of solid layers. Li et al. used imidazole as a buffer in HCl solution and the solution has a mild pH of 5.0. Upon discharge, as protons are consumed, the imidazole-acid composite will gradually release protons. The battery exhibited a high practical discharge capacity due to the utilization of small-molecule and high-concentration strong acids [43]. Other than buffered strong acids, weak acids are the better choice. Zhang et al. used acetic acid and formic acid solutions as catholytes, and found that the electrical conductivity of solid layers decreased in 100% acetic acid and formic acid. However, the electrical conductivity was not changed in formic acid-water saturated with lithium formate and increased in acetic acid–water saturated with lithium acetate. Therefore, they finally chose acetic acid–water saturated with lithium acetate as the catholyte [44]. Phosphoric acid is another weak acid applied to Li–air batteries [45]. Because of three protons in a molecule of phosphoric acid, the batteries have high specific capacity (based on Eqs. (2)). Howbeit, $Li_2HPO_4$ and $Li_3PO_4$ have very low solubility in water, which would deposit and clog air cathodes with the consumption of protons. The polarization of air cathodes will increase and then lead to gradual loss of the battery efficiency. The aqueous electrolyte can endow the battery with good rate performance, but the complex construction of "hybrid" and "aqueous" batteries impedes its application.

### 3.2. Organic electrolytes

Organic electrolytes have been broadly used in alkali metal–air batteries in virtue of their relative stability to alkali metals as well as their wide electrochemical windows. Alkylcarbonate electrolytes were early used in alkali metal–air batteries [46,47]. However, organic carbonates are not suitable as electrolytes for Li–$O_2$ batteries because of its instability during cycles [48]. Subsequently, ether electrolytes were widely used in Li–$O_2$ batteries, and were considered as suitable electrolytes for Li–$O_2$ batteries. However, many reports demonstrate that these ether electrolytes were not as stable as imagined. Christopher et al. used differential electrochemical mass spectrometry to characterize the stability of tetraethylene glycol dimethyl ether (TEGDME) in Li–$O_2$ batteries. TEGDME was partially decomposed during the cycle [49]. Despite the former report, Sharon et al. applied $LiNO_3$ in ether solvents and demonstrated that the electrolyte could improve both ORR and oxygen evolution reaction (OER) activity, while the fact that the ether solutions are not really stable in Li–$O_2$ batteries cannot be neglected [50]. Zhang group firstly applied dimethyl sulfoxide (DMSO) as the electrolyte for Li–$O_2$ batteries. Superior battery performances, including high discharge capacity and low charge overpotential, were successfully obtained due to the low volatility and high stability of DMSO [51]. Marshall et al. investigated the characteristic of DMSO in Li–$O_2$ batteries, and they suggested that DMSO is chemically and electrochemically stable on the surface of $Li_2O_2$ with both experimental and theoretical evidence [51]. Straight-chain alkyl amides, such as *N*,*N*-dimethylacetamide (DMA), are one of a few classes of polar, aprotic solvents that resist chemical degradation in the $O_2$ electrode. But these solvents do not form a stable SEI film on Li metal anodes. Walker et al. found that stable SEI film formed by employing $LiNO_3$ in DMA [20]. When fluorinated amides were used as additives in DMA, stable SEI film also formed on the surface of Li metal [52]. Quantum chemical calculations indicated that α-fluorinated alkyl amides could be reduced on the Li surface to form insoluble LiF with no or little activation energy. LiF plays a very important role in stabilizing SEI film.

Kim et al. investigated two types of Na–air batteries with carbonate and ether electrolytes, and found that the formation and decomposition of $Na_2CO_3$ was responsible for the cyclic process in the carbonate-based battery. In contrast, $Na_2O_2\cdot 2H_2O$ and NaOH were the main products in the ether electrolyte [53]. Additionally, Janek group used diethylene glycol dimethyl ether (DEGDME)-based electrolytes in Na–air batteries. The batteries showed very small overpotential during the charge process due to the formation of crystalline sodium superoxide ($NaO_2$) as the discharge product via a one-electron step [54]. Zhao et al. also investigated Na–air batteries with various electrolytes, and their results showed that carbonated-based electrolytes (EC/PC) are not stable in the batteries since the discharge products primarily consist of $Na_2CO_3$ coupled with sodium alkylcarboxylate, while the most discharge deposit is $NaO_2$ in the batteries with stable ether-based electrolytes [55]. Fig. 4 summarizes the possible side reactions of different electrolytes in Na–air batteries. It can be seen that carbonate and ether based electrolytes can be attacked by $O_2^{\cdot}$. Ether-based electrolytes are relatively stable, which are also applied to K–air batteries. Currently, 1,2-dimethoxyethane (DME) was used as the electrolyte solvent for K–air batteries and showed good stability [56,57]. Non-aqueous electrolytes inspire high hope in alkali metal–air batteries as widely studied electrolytes. However, the present electrolytes have been proved more or less decomposition during cycling. It is urgent to find more stable electrolytes.

### 3.3. Room temperature ionic liquids

Room temperature ionic liquids (RTILs) are low temperature molten salts, composed entirely of organic cations and anions. They are used as new electrolytes for alkali metal–air batteries, since RTILs are extremely non-volatile.

Takechi et al. examined the stability of several solvents against superoxide anion radicals ($O_2^{\cdot}$) by adding potassium superoxide ($KO_2$) into the electrolyte for Li–air batteries. Among them, *N*-methyl-*N*-propylpiperidinium bis(trifluoromethanesulfonyl)imide (PP13TFSI) was the most stable and suitable solvent for the electrolyte of Li–air batteries [58]. Subsequently, Guo group used PP13TFSI-$LiClO_4$ as the electrolyte for Li–$O_2$ batteries. The retention of discharge capacity can reach 56% after 20 cycles when the maximum capacity was limited to 800 mAh $g^{-1}$ [59]. Allen et al. used 1-

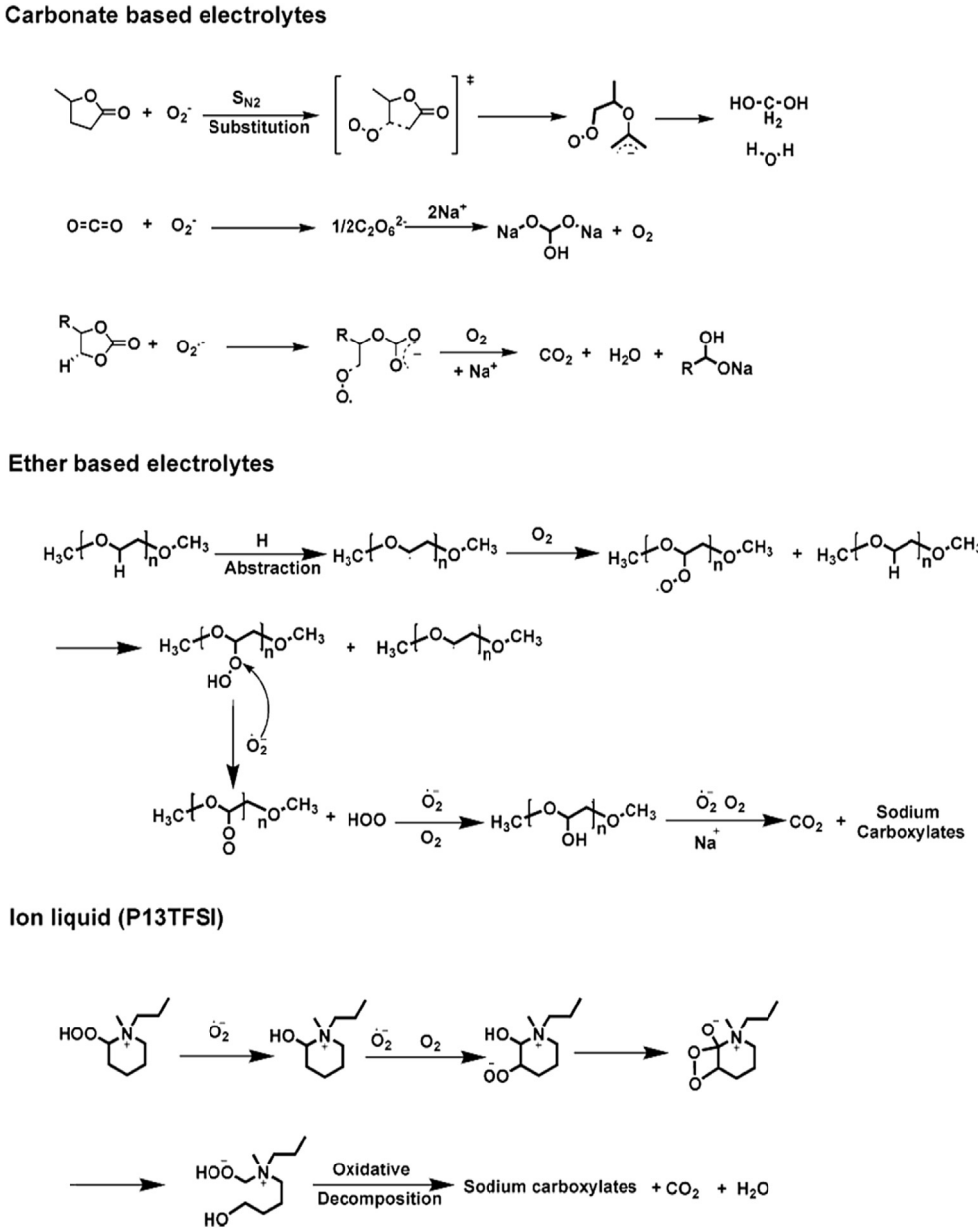


Fig. 4. Possible reactions of different electrolytes in Na–air batteries [49,51].

ethyl-3-methylimidazolium bis(triflouromethanesulfonyl) imide (EMIMTFSI) as the solvent for Li–air batteries. One-electron $O_2/O_2^-$ reversible couples existed in neat EMIMTFSI, while the presence of $Li^+$ significantly changes the ORR mechanism with the initial $LiO_2$ decomposed to $Li_2O_2$ [60]. Monaco et al. developed Li–air batteries with *N*-butyl-*N*-methylpyrrolidinium bis(trifluoromethanesulfonyl) imide (Pyr14TFSI):LiTFSI of the ratio of 9:1 as the electrolyte, and a novel configuration of flow-Li/$O_2$ batteries was designed. The batteries could be operated at high rates [61]. Skyamal et al. reported Na–air batteries with 1-methyl-3-propylimidazolium bis(trifluoromethanesulfone)imide (PMIMTFSI) as the electrolyte, and $CO_2$ and $O_2$ (40:60) as the reactant gas. Compared with TEGDME-based electrolytes, there is no difference in discharge capacities between them, but the discharge products are different. For RTILs, the discharge product is $Na_2C_2O_4$, while both $Na_2C_2O_4$ and $Na_2CO_3$ are observed in TEGDME [62]. The RTIL of PP13TFSI was firstly introduced to Na–air batteries as the electrolyte solvent, but it seemed not very stable in Na–air batteries [55]. Recently, many researches have focused on the stability of RTILs. Imidazolium-based ionic liquids were found to react with $O_2^-$ [63], while those with quaternary ammonium cations were found to be more stable [64]. Thus, piperidinium and pyrrolidinium based ionic liquids are more prospective. However, by employing the UV–vis screening method more recently, it has been found that Pyr14TFSI could react with $O_2^-$ [65]. Furthermore, Pyr14TFSI is reduced on metallic lithium, producing substantial amount of alkenes and amines [66]. In addition, Das et al. found that both

pyrrolidinium- and piperidinium-based ionic liquids are not stable in Li–air batteries [67]. Therefore, it is greatly needed to search for stable RTILs for alkali metal–air batteries.

### 3.4. Solid-state electrolytes

Solid-state electrolytes have been pursued for decades, which were originally proposed to improve the safety of Li ion batteries. Recently, they have been used in metal–air batteries. Solid-state electrolytes can be separated into two types: solid organic electrolytes and solid inorganic electrolytes.

Solid organic electrolytes are mainly polymers. Interestingly, the first reported Li–$O_2$ batteries used polyacrylonitrile (PAN)-based polymer electrolytes. The electrolyte contained carbonate-based solvents, which later became known to decompose irreversibly in Li–$O_2$ batteries [68]. Afterward, poly(ethylene oxide) (PEO) electrolyte was widely used in Li–$O_2$ batteries. Scrosati et al. used a $ZrO_2$-added PEO-based polymer composite electrolyte in Li–$O_2$ batteries. The addition of $ZrO_2$ was used to lower the internal resistance, but the batteries failed even at very low current densities [69]. To improve the performance of the batteries, Balaish et al. operated the Li–$O_2$ batteries at 80 °C. At high temperature, PEO had acceptable ionic conductivity. Besides, the formation of lithium-metal dendrites upon cycling can be solved at high temperature [70]. Investigations also demonstrate that PEO combined with hard polystyrene block did suppress the formation of dendrites [71]. Solid-state electrolyte has poor contact with air cathodes. To solve this problem, Nadege et al. designed 3D solid polymer electrolyte (SPE) structures incorporating with carbon nanotube (CNT) electrodes, as show in Fig. 5. Without incorporating with CNTs, the active reaction zone is restricted to the topmost surface of the electrode/SPE boundary, forming a 2D region (Fig. 5a). To compensate this, an improved SPE structure was designed (Fig. 5b). The novel structure favored the formation of an active reaction zone, where $O_2$ gas, $Li^+$ ions and electrons can interact [72]. In addition, a novel method was proposed to decrease the poor contact with air cathodes. Zhou group combined redox mediators (RMs) with a polymer electrolyte, which is in favor of a decrease of interfacial resistance between $Li_2O_2$ and the gel polymer electrolyte [22]. Lately, Shao-Horn group investigated the stability of PEO, and observed that applying potentials above 3 V, which is typically required for the charging process of Li–$O_2$ batteries, will increase the rate of PEO autooxidation in an oxygenated environment [73]. Therefore, they proposed that stable electrolytes not based on PEO should be developed. The electrolyte of polypropylene (PP)-supported poly(methylmethacrylate) (PMMA)-blend-poly(styrene) (PSt) with doping nanofumed $SiO_2$ was prepared for Li–$O_2$ batteries. The batteries with this kind of SPE revealed enhanced cyclic stability, which is predominantly beneficial from the absence of the blocked pores caused by the flooding liquid electrolyte and enhancement of the oxygen diffusion in cathodes, together with the suppression of dendrite formation during cycling [74].

Up to now, solid inorganic electrolytes applied in alkali metal–air batteries are glass-ceramic (GC) and NASICON-type lithium ion conductor ceramics. In 2009, Abraham et al. proposed solid-state Li–air batteries, which are composed of a Li metal anode, a highly Li-ion conductive solid electrolyte membrane laminate fabricated from GC and polymer-ceramic composites, and an air cathode. The batteries exhibited excellent thermal stability and rechargeability in the temperature range of 30–105 °C [75]. Subsequently, Zhou group assembled batteries with polymer and Li–Al–Ti–$PO_4$

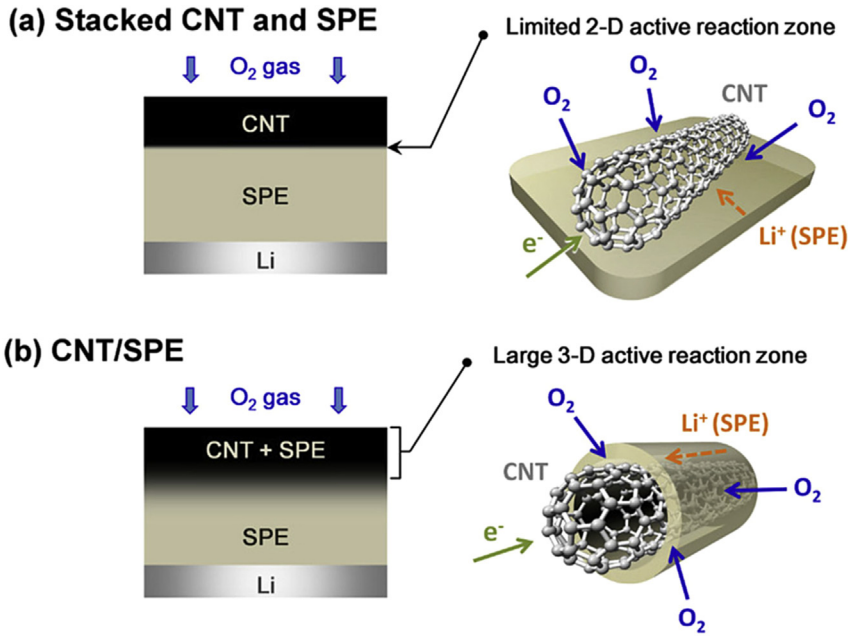


Fig. 5. Schematics of (a) limited 2-D active reaction zone in conventional CNT and SPE sandwiched structure and (b) enlarged 3-D active reaction zone in 3-D CNT/SPE architecture [68].

(LATP) as solid-state electrolytes. The polymer membrane was used to avoid LATP directly contacting with Li metal, in order to protect $Ti^{4+}$ from being reduced to $Ti^{2+}$ by lithium. The batteries showed finite cycles at low current density because of their high interfacial resistance [76]. To reduce the interfacial resistance of batteries, Liu et al. designed batteries without the buffering polymer membrane, and prepared NASICON-type $Li_{1.5}Al_{0.5}Ge_{1.5}(PO_4)_3$ (LAGP) as electrolytes. In the LAGP ceramics, $Al^{3+}$ substitution for $Ge^{4+}$ introduces additional lithium in the structure and improves the total lithium ion conductivity. In addition, the LAGP ceramics exhibited good and relative stability in contact with Li metal and in air atmosphere, respectively [77]. More recently, Zhu et al. have designed solid-state batteries with carbon coated porous LATP as cathodes, as shown in Fig. 6. The uppermost dense layer of the integrated LATP structure (Fig. 6b) served as the electrolyte, while the bottom porous layer (Fig. 6c) served as the cathode support. The carbon nanoparticles coated on LATP can be seen clearly (Fig. 6d). The cathode was then protected with silicone-oil film, which blocked water vapor and carbon dioxide from reaching reaction sites. This battery can operate in ambient air at 5000 mAh $g^{-1}$ for 50 cycles [78]. All solid-state batteries are the promising candidate for future power supply. Currently, the low ionic conductivity is the main bottleneck of the development of all solid-state batteries. Therefore, it has great significance to improve the ionic conductivity of solid-state electrolytes.

### 3.5. Liquid phase catalysts

At present, the most commonly used catalysts in metal–air batteries are loaded on the air cathodes, and act only on the surface of discharge products ($Li_2O_2$, $Na_2O$, $Na_2O_2$, or $K_2O$) during charge process, which we can call them heterogeneous catalysts. Liquid phase catalysts can dissolve in the electrolyte and promote the OER/ORR on a much larger scale. The liquid phase catalyst is based on the reversible redox pair $RM \rightleftharpoons RM^+ + e^-$, and provide oxidative attack at the much larger interphase between discharge products and the liquid electrolyte.

Up to now, the investigations on liquid phase catalysts focus on promoting the OER process. Most of them are small molecules, containing iodides [79], tetrathiafulvalene (TTF) [80], nitroxides [81], and phenothiazine [82], among which iodides are widely studied. Kang et al. firstly combined LiI in TEGDME with porous carbon nanotube fibrils for Li–$O_2$ batteries. The batteries displayed superior cyclability over 900 cycles even at the current of 2 A $g^{-1}$ with the capacity cutoff of 1000 mAh $g^{-1}$. In the catalytic process, $I^-$ was oxidized to $I^{3-}$, and then $O_2$ was generated from $Li_2O_2$ by the oxidation of $I^{3-}$ [79]. By using LiI to incorporate a photo-electrode with the oxygen electrode, the overpotential during the charge process can be drastically reduced. This novel method was first proposed by Wu group [83]. The mechanism of the photo-assisted charge process is shown in Fig. 7. On charging under illumination, the photo-excited dye molecules inject electrons into the conduction band of $TiO_2$ and are regenerated by oxidizing $I^-$ to $I_3^-$. $I_3^-$ subsequently diffuses to the oxygen electrode, oxidizes the solid $Li_2O_2$ to $O_2$ and is reduced back to complete a full redox cycle. Liu et al. also used this method to reduce the overpotenial. They used g-$C_3N_4$ as photocatalyst, which remarkably reduced the charge voltage to 1.9 V, which is even much lower than the discharging voltage [84]. Sun et al. also investigated the effect of LiI in Li–$O_2$ batteries, and they found that the concentration of LiI influences its catalytic activity. At high concentrations, the presence of the salt

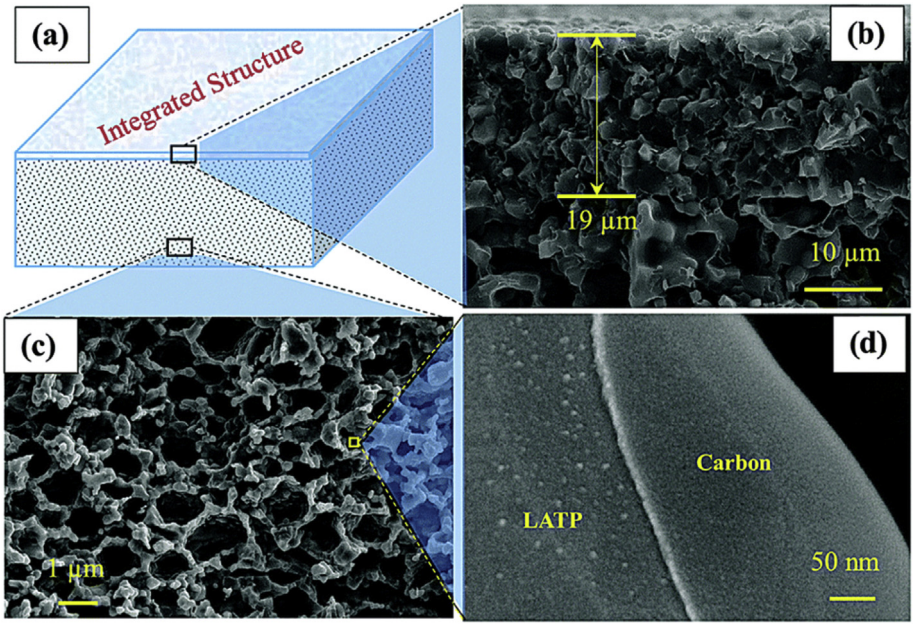


Fig. 6. (a) Schematic illustration of the proposed integrated structure with a dense LATP membrane and a porous LATP cathode-support. SEM images of (b) a dense LATP membrane seamlessly connected with (c) a porous LATP cathode-support, and (d) a carbon nanoparticle-coated LATP cathode [75].

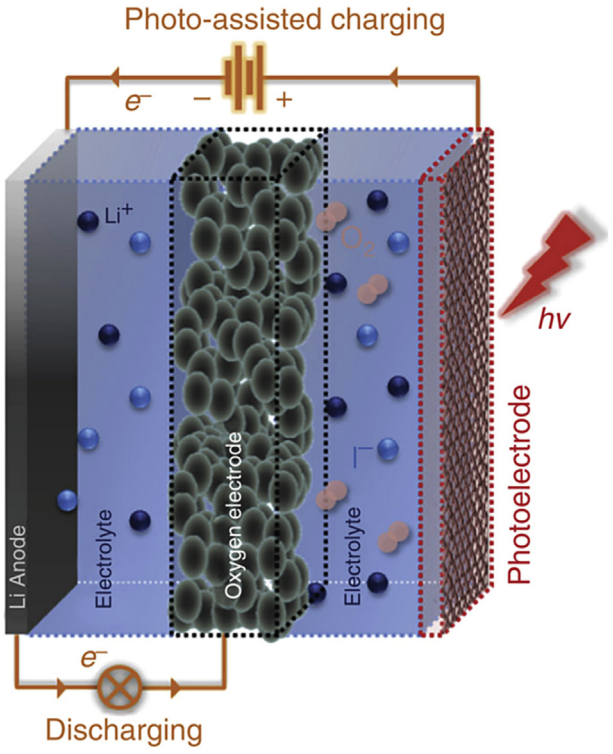


Fig. 7. The mechanism of the photo-assisted charging process of Li–$O_2$ batteries.

promotes a side reaction that forms LiOH as a major product. In turn, at low concentrations, the discharge product is $Li_2O_2$ [85]. Due to the significant effect of $I^-$, it was also introduced to Na–air batteries. Yin et al. dissolved NaI into the electrolyte, and found that the batteries with NaI can operate at lower charge voltage and exhibit a long-life cycling performance [86]. However, the volatilization of iodine would result in the deterioration of the electrochemical performance. They investigated another liquid phase catalyst, ferrocene. This new nonvolatile and soluble catalyst endows the batteries with enhanced performance than NaI [87]. Interestingly, even $H_2O$ was found to be a liquid phase catalyst for metal–air batteries, which will be discussed in detail in Section 5.

## 4. Air cathodes

Air cathodes also play an important role in alkali metal–air batteries. In general, the air cathode should own three features: massive and connected channels for the diffusion of gas and deposition of discharge product, good electrical conductivity to facilitate the electron transportation, and highly catalytic activity for ORR and OER. Carbon based materials are commonly used in alkali metal–air batteries due to their excellent electrical conductivity and high porosity. The porous structure and good electrical conductivity of the air cathode facilitate the transport of gases, the immersion of electrolytes and electron transfer. After all, the air cathode is the place where $O_2$ undergoes redox reactions. Unfortunately, the reaction kinetics of ORR and OER is sluggish, especially the latter. Various catalysts loaded carbon substrates as well as heteroatom modified carbon materials have been widely explored as air cathodes. There have been several insightful reviews on ORR/OER bifunctional catalysts for metal–air batteries recently [88–90], so we will not mention much in this respect. However, there is very little attempt focusing on the structure and stability of cathodes, which is significant for metal–air batteries. Therefore, in the section of air cathodes, we keep our eyes on this topic.

### 4.1. Carbon cathodes

Carbon based cathodes for metal–air batteries have been largely studied, and obviously the nanostructured carbon configurations can effectively enhance the kinetics of the electrochemical process. Recently, graphene as a star material has attracted great attention. It was also used in metal–air batteries. Graphene nanosheets (GNSs) were used as cathode substrates for Na–air batteries. The high surface area of graphene can efficiently alleviate the blockage of oxygen diffusion channels due to the discharge product aggregation, and the batteries can deliver high initial discharge capacity. However, the capacity faded with cycling significantly, which was caused by the accumulation of insoluble discharge products in the porous network of the GNS cathode [91]. By electrochemical leavening of graphite papers, porous graphene foams formed. Upon application to Li–air batteries, the batteries delivered a round-trip efficiency of up to 80% with a stable discharge voltage at 2.8 V and a stable charge voltage below 3.8 V for 20 cycles [92]. Highly ordered and ultra-long CNTs could grow on permeable Ta foil substrates via thermal chemical vapor deposition (CVD). The composite had highly ordered structure with larger specific surface area and fewer surface defects, which leads to enhanced performance of Li–air batteries when used as cathodes. Furthermore, vertically aligned CNTs were used in Na–air batteries, and the batteries only had a low overpotential of 0.2 V, and can maintain 90% energy efficiency up to 100 cycles [93]. CNTs can also be designed as films. The hierarchically porous CNT film was prepared by a template method; there were numerous interconnected large tunnels after removing the template. Then the film was applied to Li–air batteries, which exhibited excellent electrochemical performance by virtue of the unique bimodal design for porosity [94]. Carbon nanofibers (CNFs) have similar shape to CNTs, which can also form 3D contacted networks. Nie et al. utilized free-standing CNFs to assemble thin webs. A hierarchically porous structure with micron-sized pores and mesopores was obtained. Directly using it as the cathode, the battery showed reduced overpotential [95].

Additionally, other nanostructured carbon-based cathodes have been obtained. Ordered mesoporous carbon (OMC) was synthesized and evaluated as nanostructured conductive matrix to host low-conductivity products generated during the discharge of Na–air batteries. OMC has high specific surface area which can store more discharge products [96]. In another work, Sun et al. prepared cathodes based on mesoporous

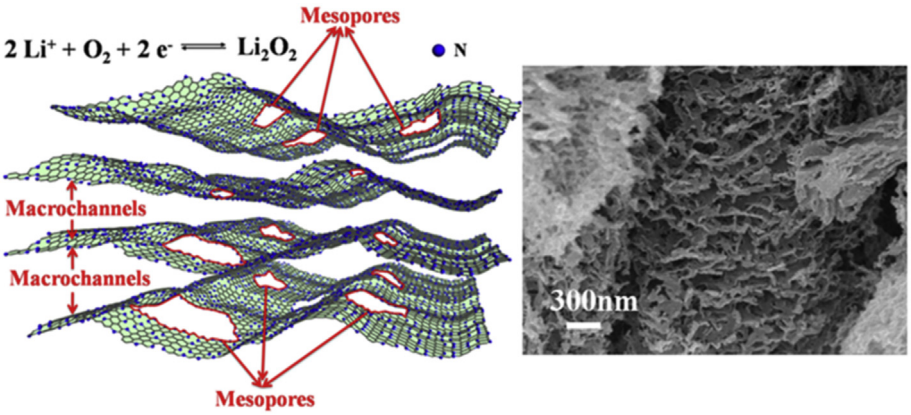


Fig. 8. Schematic illustration and SEM image of hierarchical carbon-nitrogen material with both macrochannels and mesopores [86].

carbon nanocubes (MCC) by a hard template method through a CVD process, and large amount of macropores also formed between carbon nanocubes, which can facilitate the transport of electrolytes and oxygen [97]. Zhang et al. prepared hierarchical carbon–nitrogen architectures with both mesopores and macrochannels (Fig. 8) as excellent cathodes for Li–$O_2$ batteries. The hierarchical pore structures (ordered mesopores and macrochannels) provide optimized oxygen transport network and adequate space for the deposition of $Li_2O_2$ [98]. Up to date, only porous carbon cathodes were used for K–air batteries [28,56,57].

Although carbon-based cathodes have many good performances, their suitability is disputed as air cathodes due to the concern on chemical stability. Thotiyl et al. found that carbon is relatively stable below 3.5 V during both the discharge and charge processes, but unstable above 3.5 V in the presence of $Li_2O_2$ [99]. By employing a carbon-13 isotope ($^{13}C$) cathode, McCloskey and Speide discovered that carbon cathodes can react with the discharge product $Li_2O_2$ to form approximately a monolayer of $Li_2CO_3$ at the C–$Li_2O_2$ interface [19].

### 4.2. Non-carbon cathodes

The challenges from chemical instability of carbon cathodes are not totally resolved. Finding suitable alternative cathodes to carbon is a feasible way. Thotiyl et al. reported porous TiC as cathode materials for Li–air batteries since TiC has good electronic conductivity and low density. During the cycling, a passivated "$TiO_2$-rich" surface layer formed on TiC which inhibits unwanted side reactions of the electrolyte. The batteries maintained the capacity retention of 98% after 100 cycles [100]. After that, nanoporous $Mo_2C$ nanofibers with high surface areas were generated by a thermochemical approach and used in Li–air batteries [101]. As we know, gold is very stable with high electrical conductivity. NPG is a great cathode for metal–air batteries, which has been used in both Li–air and Na–air batteries [18,34,102]. Xu et al. have recently demonstrated Au with 3D meshy structure as cathodes for Li–air batteries. The structure facilitated the transport of oxygen and electrolytes, and thus enhanced kinetic process of the batteries. The chemical stability of Au reduced side reactions [102].

Even though carbon-alternative cathodes have enhanced chemical stability, the improvement on the mechanical stability of carbon-alternative cathodes should be noted.

## 5. Reactant gases

Up to the present, the vast majority of alkali metal–air batteries studied in the literature use $O_2$ as the reactant gas instead of air. Because there are moisture and $CO_2$ in ambient air, which can introduce a series of side reactions in the battery. Insulating species such as alkali metal hydroxide and alkali metal carbonate can form at the cathode, making the batteries less rechargeable or even causing the death of batteries. To realize true alkali metal–air batteries, the effects of $CO_2$ and moisture must be taken into account. It is possible to remove these compositions in a practical metal–air battery by adding a gas filtration system to remove $H_2O$ and $CO_2$ from ambient air or by including an on-board storage tank to deliver pure oxygen as desired during battery operation [78,103]. However, there is no superior filtrating system that can efficiently separate $H_2O$ and $CO_2$ from air. In addition, the introduction of these additional components leads to substantial increase in the weight and cost of metal–air systems, which cancel out the most important advantages of metal–air batteries. However, the effects of $H_2O$ and $CO_2$ on the performance of metal–air batteries are not completely clear.

The effect of $CO_2$ on Li–$O_2$ was firstly studied by Takechi et al., the mixed gas of $O_2$ and $CO_2$ was introduced to Li–air batteries. The discharge capacity reached three times as much as that of a non-aqueous Li–air ($O_2$) battery when the gas consisted of 50% $CO_2$ [104]. The same phenomenon was also discovered in Na–air batteries. When utilizing $CO_2$ and $O_2$ (40:60) as the reactant gas, the discharge capacities were 2.1 and 2.6 times higher than the corresponding Na–$O_2$ battery with PP13TFSI and TEGDME-based electrolytes, respectively. The discharge product was $Na_2C_2O_4$ in the PP13TFSI based electrolyte, while both $Na_2C_2O_4$ and $Na_2CO_3$ are observed in the TEGDME electrolyte [62]. It was perhaps

caused by different reactions between $O_2^{\cdot}$ and $CO_2$. When the discharge product is carbonate, the reactions occur as follows:

$$4O_2 + 4e^- \rightarrow 4O_2^{\cdot -} \quad (3)$$

$$O_2^{\cdot -} + CO_2 \rightarrow CO_4^{\cdot -} \quad (4)$$

$$CO_4^{\cdot -} + CO_2 \rightarrow C_2O_6^{\cdot -} \quad (5)$$

$$C_2O_6^{\cdot -} + CO_2 \rightarrow C_2O_6^{2-} + O_2 \quad (6)$$

$$C_2O_6^{2-} + 2O_2^{\cdot -} + 4M^+ \rightarrow 2M_2CO_3 + 2O_2 \quad (7)$$

For oxalate, the reactions are demonstrated as below.

$$O_2 + 2e^- \rightarrow O_2^{2-} \quad (8)$$

$$CO_2 + O_2^{2-} \rightarrow CO_4^{2-} \quad (9)$$

$$CO_4^{2-} + CO_2 + 2M^+ \rightarrow M_2C_2O_4 \quad (10)$$

Although $CO_2$ contamination increases the discharge capacity of the battery, the presence of $CO_2$ during discharge dramatically influences the electrochemical process because high overpotentials are needed to decompose $Li_2CO_3$ during the charge of the battery [105]. Kim et al. studied Li–$O_2$/$CO_2$ batteries with DME and DMSO electrolytes, and discovered that $Li_2O_2$ is the discharge product in low dielectric electrolytes (DME) while $Li_2CO_3$ in high dielectric electrolytes (DMSO). Moreover, they found reversible formation and decomposition of $Li_2CO_3$ in DMSO. The batteries were stably cycled for over 20 cycles [106]. Recently, it has been reported that the battery could cycle with a moderate discharge capacity in pure $CO_2$, which is called rechargeable Li–$CO_2$ batteries [107]. The theoretical voltage is about 2.8 V based on the reaction: $4Li + 3CO_2 \rightarrow 2Li_2CO_3 + C$ [108]. After that, in order to increase the capacity and cycling performance of Li–$CO_2$ batteries, Zhou group added graphene or CNTs to cathodes to increase the performances of Li–$CO_2$ batteries [109,110]. Although Li–$CO_2$ batteries were investigated only at low current densities (50–100 mAh $g^{-1}$), a growing consensus is that rechargeable Li–$CO_2$ batteries offer great promise by combining carbon capture and energy technology.

The amount of water in the air can reach up to 4% depending on humidity, and is generally much greater than that of $CO_2$ (400 ppm) in ambient air. The effect of water on alkali metal–air batteries should be considered seriously. Meini et al. compared the discharge performance of Li–$O_2$ batteries in water-free electrolyte with water-contaminating one, and the latter got an increased first discharge capacity up to one order of magnitude. The authors assumed that $O_2^{\cdot -}$ reacts preferentially with trace water rather than forming $LiO_2$ followed by disproportionation to $Li_2O_2$. The products could be slightly soluble in the electrolyte and diffuse into the bulk of the solution [111]. A detailed study by Aetukuri et al. also showed a clear and consistent increase in the discharge capacity as a function of water content. According to X-ray diffraction (XRD) analysis, it proved that $Li_2O_2$ formed during the discharge process. Scanning electron microscope (SEM) image showed that toroid-shaped $Li_2O_2$ enlarged with increasing the water content in electrolytes. Through further quantitative analysis, the authors confirmed that $H_2O$ can increase the solubility of $LiO_2$ in the electrolyte, which makes the growth of $Li_2O_2$ according to the solution mechanism. The mechanism for the growth of $Li_2O_2$ in presence of water is provided in Fig. 9 [112]. $LiO_2$* is the intermediate species forming in the discharge process, where * refers to a surface-adsorbed species, (s) indicates solid and (sol) indicates a species in solutions. $LiO_2$* is insoluble in the absence of water, which results in the formation of $Li_2O_2$ film. For the electrolyte with water, the solubility $LiO_2$* increased. $Li^+$ (sol) and solvated $O_2^-$ ($O_2^-$ (sol)) in the electrolyte triggered a solution pathway leading to the growth of toroids. Inspired by this, Zhou group used water as the catalyst for Li–$O_2$ batteries [113]. Similar conclusion was also obtained in Na–$O_2$ batteries, and Nazar group found that water acted as phase-transfer in Na–$O_2$ batteries. Quasi-amorphous $NaO_2$ formed in the absence of water. On the contrary, cubic $NaO_2$ formed with trace water in the electrolyte. As shown in Fig. 10, water in the electrolyte promotes the growth of $NaO_2$ by the solution mechanism [114]. Very recently, Liu et al. have reported the cycling Li–$O_2$ batteries via LiOH formation and decomposition. LiOH formed because of moisture in the atmosphere. The batteries showed amazing performance, which

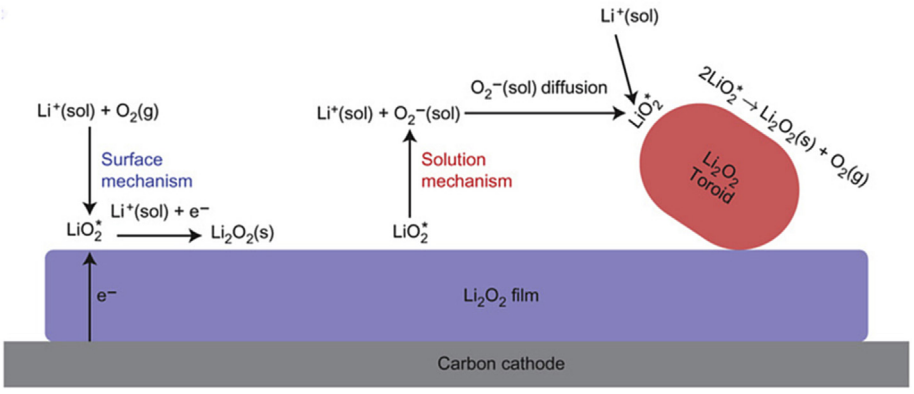


Fig. 9. The mechanism for the growth of $Li_2O_2$ with or without water in the electrolyte [102].

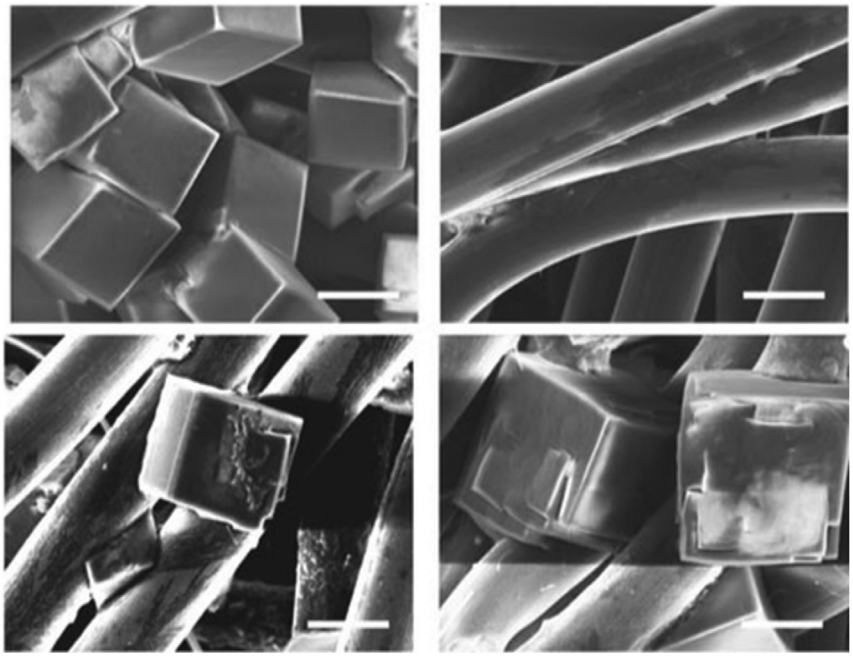

Fig. 10. Cubic $NaO_2$ forming during the discharge process [103].

can stably cycle over 300 cycles at 5 A $g^{-1}$ with limited capacity of 5000 mA $g^{-1}$. The electrochemical performance of the battery is shown in Fig. 11 [115]. Tremendous efforts had been dedicated in the influences of $CO_2$ and moisture, but the mechanism is not clear completely, and further studies are required.

## 6. Conclusion and outlook

There has been fantastic progress in the area of alkali metal–air batteries in recent years. Promising electrochemical performance and high energy density are factors that have driven research interest in these batteries. The batteries would

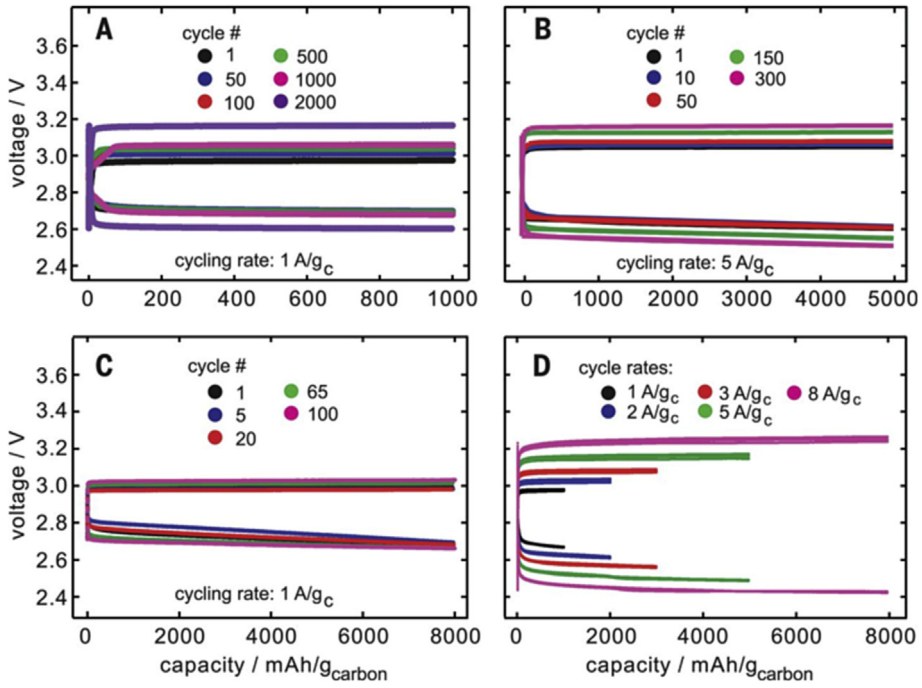


Fig. 11. Discharge/charge curves for Li–$O_2$ batteries using rGO electrodes and a 0.05 M LiI/0.25 M LiTFSI/DME electrolyte with capacity limits of 1000 mA h/gc (A), 5000 mA h/gc (B), and 8000 mA h/gc (C), as a function of rate (D); three cycles were performed for each rate in (D). The battery cycle rate is based on the mass of rGO; i.e., 5 A/gc is equivalent to 0.1 mA/$cm^2$ [104].

offer great benefit if they can be harnessed to their full potential. Metal anodes, electrolytes and air cathodes are basic parts constituting alkali metal–air batteries, which are crucial for the performance of batteries. Dendrite, stability and volatility of electrolytes, and sluggish kinetic processes of ORR and OER are consistent issue plaguing researchers. Great progress has been made in all three parts in recent years though big challenges still need to be confronted.

All solid-state metal–air batteries avoid the stability and volatility of electrolytes and even suppress the growth of dendrites, and would be one of the promising future directions of reversible metal–air batteries. Although the low ionic conductivity of solid-state electrolytes at room temperature puts sand in the wheels of the development of solid-state metal–air batteries, great hope exists to increase the ionic conductivity of both ceramic and polymer electrolytes. There is little information available about metal–air batteries with solid electrolytes, and few investigations on the detailed characterization of ORR and OER in solid-based system, which deserve much attention. Further work should focus on the development of all solid-state metal–air batteries.

In addition, the effect of reactant gases should be deeply studied. $CO_2$ and moisture in the air were considered to be harmful in the early stage of research. But in recent studies, it seems that $CO_2$ and moisture have some positive effects on the performance of alkali metal–air batteries. Moreover, Li–$CO_2$ batteries have been developed. Currently, there is no thorough elaboration on the effect of $CO_2$ and moisture in alkali metal–air batteries. Further fundamental understanding of the reaction mechanisms of metal–$CO_2$ batteries is required.

## Conflict of interest

We declare that we have no conflict of interest.

## Acknowledgments

This work was supported by NSFC (21473094 and 21421001) and MOE Innovation Team (IRT13022) in China. The authors also thank Mao-Lin Li for his help in the preparation of figures.

## References

[1] J.-M. Tarascon, M. Armand, Nature 414 (2001) 359–367.
[2] M.S. Whittingham, Chem. Rev. 104 (2004) 4271–4302.
[3] B. Dunn, H. Kamath, J.-M. Tarascon, Science 334 (2011) 928–935.
[4] J.B. Goodenough, Y. Kim, Chem. Mater. 22 (2009) 587–603.
[5] C. Liu, F. Li, L.P. Ma, H.M. Cheng, Adv. Mater. 22 (2010) E28–E62.
[6] Z. Yang, J. Zhang, M.C. Kintner-Meyer, X. Lu, D. Choi, J.P. Lemmon, J. Liu, Chem. Rev. 111 (2011) 3577–3613.
[7] J.H. Williams, A. DeBenedictis, R. Ghanadan, A. Mahone, J. Moore, W.R. Morrow, S. Price, M.S. Torn, Science 335 (2012) 53–59.
[8] A. Taniguchi, N. Fujioka, M. Ikoma, A. Ohta, J. Power Sources 100 (2001) 117–124.
[9] P.G. Bruce, S.A. Freunberger, L.J. Hardwick, J.M. Tarascon, Nat. Mater. 11 (2012) 19–29.
[10] D. Linden, T.B. Reddy, Handbook of Batteries, McGraw-Hill Professional, 2001.
[11] T. Shiga, Y. Hase, Y. Kato, M. Inoue, K. Takechi, Chem. Commun. 49 (2013) 9152–9154.
[12] T. Hibino, K. Kobayashi, M. Nagao, J. Mater. Chem. A 1 (2013) 14844.
[13] E. Mengeritsky, P. Dan, I. Weissman, A. Zaban, D. Aurbach, J. Electrochem. Soc. 143 (1996) 2110–2116.
[14] J.K. Stark, Y. Ding, P.A. Kohl, J. Electrochem. Soc. 158 (2011) A1100–A1105.
[15] G.H. Lane, A.S. Best, D.R. MacFarlane, M. Forsyth, A.F. Hollenkamp, Electrochim. Acta 55 (2010) 2210–2215.
[16] F. Ding, W. Xu, G.L. Graff, J. Zhang, M.L. Sushko, X. Chen, Y. Shao, M.H. Engelhard, Z. Nie, J. Xiao, J. Am. Chem. Soc. 135 (2013) 4450–4456.
[17] R. Younesi, M. Hahlin, M. Roberts, K. Edström, J. Power Sources 225 (2013) 40–45.
[18] Z. Peng, S.A. Freunberger, Y. Chen, P.G. Bruce, Science 337 (2012) 563–566.
[19] R. Younesi, M. Hahlin, K. Edstrom, ACS Appl. Mater. Interfaces 5 (2013) 1333–1341.
[20] W. Walker, V. Giordani, J. Uddin, V.S. Bryantsev, G.V. Chase, D. Addison, J. Am. Chem. Soc. 135 (2013) 2076–2079.
[21] H. Lee, D.J. Lee, J.-N. Lee, J. Song, Y. Lee, M.-H. Ryou, J.-K. Park, Y.M. Lee, Electrochim. Acta 123 (2014) 419–425.
[22] M. Roberts, R. Younesi, W. Richardson, J. Liu, J. Zhu, K. Edstrom, T. Gustafsson, ECS Electrochem. Lett. 3 (2014) A62–A65.
[23] P. Hartmann, C.L. Bender, J. Sann, A.K. Durr, M. Jansen, J. Janek, P. Adelhelm, Phys. Chem. Chem. Phys. 15 (2013) 11661–11672.
[24] J. Hassoun, H.-G. Jung, D.-J. Lee, J.-B. Park, K. Amine, Y.-K. Sun, B. Scrosati, Nano Lett. 12 (2012) 5775–5779.
[25] G.A. Elia, D. Bresser, J. Reiter, P. Oberhumer, Y.-K. Sun, B. Scrosati, S. Passerini, J. Hassoun, ACS Appl. Mater. Interfaces 7 (2015) 22638–22643.
[26] Z. Guo, X. Dong, Y. Wang, Y. Xia, Chem. Commun. 51 (2015) 676–678.
[27] C.L. Bender, B. Jache, P. Adelhelm, J. Janek, J. Mater. Chem. A 3 (2015) 20633–20641.
[28] W.D. McCulloch, X. Ren, M. Yu, Z. Huang, Y. Wu, ACS Appl. Mater. Interfaces (2015) 26158–26166.
[29] G. Zheng, S.W. Lee, Z. Liang, H.-W. Lee, K. Yan, H. Yao, H. Wang, W. Li, S. Chu, Y. Cui, Nat. Nanotechnol. 9 (2014) 618–623.
[30] D.J. Lee, H. Lee, J. Song, M.-H. Ryou, Y.M. Lee, H.-T. Kim, J.-K. Park, Electrochem. Commun. 40 (2014) 45–48.
[31] S.J. Kang, T. Mori, J. Suk, D.W. Kim, Y. Kang, W. Wilcke, H.-C. Kim, J. Mater. Chem. A 2 (2014) 9970.
[32] Q.C. Liu, J.J. Xu, S. Yuan, Z.W. Chang, D. Xu, Y.B. Yin, L. Li, H.X. Zhong, Y.S. Jiang, J.M. Yan, X.B. Zhang, Adv. Mater. 27 (2015) 5241–5247.
[33] X. Bi, X. Ren, Z. Huang, M. Yu, E. Kreidler, Y. Wu, Chem. Commun. 51 (2015) 7665–7668.
[34] T. Hashimoto, K. Hayashi, Electrochim. Acta 182 (2015) 809–814.
[35] S.H. Sahgong, S.T. Senthilkumar, K. Kim, S.M. Hwang, Y. Kim, Electrochem. Commun. 61 (2015) 53–56.
[36] H. Wang, D. Im, D.J. Lee, M. Matsui, Y. Takeda, O. Yamamoto, N. Imanishi, J. Electrochem. Soc. 160 (2013) A728–A733.
[37] P. He, Y. Wang, H. Zhou, J. Power Sources 196 (2011) 5611–5616.
[38] Y. Shimonishi, T. Zhang, N. Imanishi, D. Im, D.J. Lee, A. Hirano, Y. Takeda, O. Yamamoto, N. Sammes, J. Power Sources 196 (2011) 5128–5132.
[39] H. He, W. Niu, N.M. Asl, J. Salim, R. Chen, Y. Kim, Electrochim. Acta 67 (2012) 87–94.
[40] Y. Li, Z. Huang, K. Huang, D. Carnahan, Y. Xing, Energy Environ. Sci. 6 (2013) 3339–3345.
[41] S. Hasegawa, N. Imanishi, T. Zhang, J. Xie, A. Hirano, Y. Takeda, O. Yamamoto, J. Power Sources 189 (2009) 371–377.
[42] Y. Li, K. Huang, Y. Xing, Electrochim. Acta 81 (2012) 20–24.
[43] L. Li, Y. Fu, A. Manthiram, Electrochem. Commun. 47 (2014) 67–70.
[44] Y. Shimonishi, T. Zhang, P. Johnson, N. Imanishi, A. Hirano, Y. Takeda, O. Yamamoto, N. Sammes, J. Power Sources 195 (2010) 6187–6191.
[45] L. Li, X. Zhao, A. Manthiram, Electrochem. Commun. 14 (2012) 78–81.

[46] S.S. Zhang, D. Foster, J. Read, J. Power Sources 195 (2010) 1235–1240.
[47] D. Zhang, Z. Fu, Z. Wei, T. Huang, A. Yu, J. Electrochem. Soc. 157 (2010) A362–A365.
[48] S.A. Freunberger, Y. Chen, Z. Peng, J.M. Griffin, L.J. Hardwick, F. Bardé, P. Novák, P.G. Bruce, J. Am. Chem. Soc. 133 (2011) 8040–8047.
[49] C.J. Barile, A.A. Gewirth, J. Electrochem. Soc. 160 (2013) A549–A552.
[50] D. Sharon, D. Hirsberg, M. Afri, F. Chesneau, R. Lavi, A.A. Frimer, Y.-K. Sun, D. Aurbach, ACS Appl. Mater. Interfaces 7 (2015) 16590–16600.
[51] D. Xu, Z.L. Wang, J.J. Xu, L.L. Zhang, X.B. Zhang, Chem. Commun. 48 (2012) 6948–6950.
[52] V.S. Bryantsev, V. Giordani, W. Walker, J. Uddin, I. Lee, A.C.T. van Duin, G.V. Chase, D. Addison, J. Phys. Chem. C 117 (2013) 11977–11988.
[53] J. Kim, H.-D. Lim, H. Gwon, K. Kang, Phys. Chem. Chem. Phys. 15 (2013) 3623–3629.
[54] P. Hartmann, C.L. Bender, M. Vračar, A.K. Dürr, A. Garsuch, J. Janek, P. Adelhelm, Nat. Mater. 12 (2013) 228–232.
[55] N. Zhao, X. Guo, J. Phys. Chem. C 119 (2015) 25319–25326.
[56] X. Ren, Y. Wu, J. Am. Chem. Soc. 135 (2013) 2923–2926.
[57] X.D. Ren, K.C. Lau, M.Z. Yu, X.X. Bi, E. Kreidler, L.A. Curtiss, Y.Y. Wu, ACS Appl. Mater. Interfaces 6 (2014) 19299–19307.
[58] K. Takechi, S. Higashi, F. Mizuno, H. Nishikoori, H. Iba, T. Shiga, ECS Electrochem. Lett. 1 (2012) A27–A29.
[59] Z.H. Cui, W.G. Fan, X.X. Guo, J. Power Sources 235 (2013) 251–255.
[60] C.J. Allen, S. Mukerjee, E.J. Plichta, M.A. Hendrickson, K. Abraham, J. Phys. Chem. Lett. 2 (2011) 2420–2424.
[61] S. Monaco, F. Soavi, M. Mastragostino, J. Phys. Chem. Lett. 4 (2013) 1379–1382.
[62] S.K. Das, S.M. Xu, L.A. Archer, Electrochem. Commun. 27 (2013) 59–62.
[63] M.M. Islam, T. Imase, T. Okajima, M. Takahashi, Y. Niikura, N. Kawashima, Y. Nakamura, T. Ohsaka, J. Phys. Chem. A 113 (2009) 912–916.
[64] F. Mizuno, S. Nakanishi, A. Shirasawa, K. Takechi, T. Shiga, H. Nishikoori, H. Iba, Electrochemistry 79 (2011) 876–881.
[65] K.U. Schwenke, J. Herranz, H.A. Gasteiger, M. Piana, J. Electrochem. Soc. 162 (2015) A905–A914.
[66] M. Piana, J. Wandt, S. Meini, I. Buchberger, N. Tsiouvaras, H.A. Gasteiger, J. Electrochem. Soc. 161 (2014) A1992–A2001.
[67] S. Das, J. Højberg, K.B. Knudsen, R. Younesi, P. Johansson, P. Norby, T. Vegge, J. Phys. Chem. C 119 (2015) 18084–18090.
[68] K. Abraham, Z. Jiang, J. Electrochem. Soc. 143 (1996) 1–5.
[69] J. Hassoun, F. Croce, M. Armand, B. Scrosati, Angew. Chem. Int. Ed. 50 (2011) 2999–3002.
[70] M. Balaish, E. Peled, D. Golodnitsky, Y. Ein-Eli, Angew. Chem. Int. Ed. 54 (2015) 436–440.
[71] E. Peled, D. Golodnitsky, G. Ardel, V. Eshkenazy, Electrochim. Acta 40 (1995) 2197–2204.
[72] N. Bonnet-Mercier, R.A. Wong, M.L. Thomas, A. Dutta, K. Yamanaka, C. Yogi, T. Ohta, H.R. Byon, Sci. Rep. 4 (2014) 7127.
[73] J.R. Harding, C.V. Amanchukwu, P.T. Hammond, Y. Shao-Horn, J. Phys. Chem. C 119 (2015) 6947–6955.
[74] J. Yi, X. Liu, S. Guo, K. Zhu, H. Xue, H. Zhou, ACS Appl. Mater. Interfaces 7 (2015) 23798–23804.
[75] B. Kumar, J. Kumar, R. Leese, J.P. Fellner, S.J. Rodrigues, K.M. Abraham, J. Electrochem. Soc. 157 (2010) A50–A54.
[76] H. Kitaura, H. Zhou, Adv. Energy Mater. 2 (2012) 889–894.
[77] Y. Liu, B. Li, H. Kitaura, X. Zhang, M. Han, P. He, H. Zhou, ACS Appl. Mater. Interfaces 7 (2015) 17307–17310.
[78] X. Zhu, T. Zhao, Z. Wei, P. Tan, L. An, Energy Environ. Sci. 8 (2015) 3745–3754.
[79] H.D. Lim, H. Song, J. Kim, H. Gwon, Y. Bae, K.Y. Park, J. Hong, H. Kim, T. Kim, Y.H. Kim, X. Lepro, R. Ovalle-Robles, R.H. Baughman, K. Kang, Angew. Chem. Int. Ed. 53 (2014) 3926–3931.
[80] Y. Chen, S.A. Freunberger, Z. Peng, O. Fontaine, P.G. Bruce, Nat. Chem. 5 (2013) 489–494.
[81] B.J. Bergner, A. Schuermann, K. Peppler, A. Garsuch, J. Janek, J. Am. Chem. Soc. 136 (2014) 15054–15064.
[82] N. Feng, P. He, H. Zhou, ChemSusChem 8 (2015) 600–602.
[83] M. Yu, X. Ren, L. Ma, Y. Wu, Nat. Commun. 5 (2014) 5111.
[84] Y. Liu, N. Li, S. Wu, K. Liao, K. Zhu, J. Yi, H. Zhou, Energy Environ. Sci. 8 (2015) 2664–2667.
[85] W.-J. Kwak, D. Hirshberg, D. Sharon, H.-J. Shin, M. Afri, J.-B. Park, A. Garsuch, F.F. Chesneau, A.A. Frimer, D. Aurbach, J. Mater. Chem. A 3 (2015) 8855–8864.
[86] W.-W. Yin, Z. Shadike, Y. Yang, F. Ding, L. Sang, H. Li, Z.-W. Fu, Chem. Commun. 51 (2015) 2324–2327.
[87] W.-W. Yin, J.-L. Yue, M.-H. Cao, W. Liu, J.-J. Ding, F. Ding, L. Sang, Z.-W. Fu, J. Mater. Chem. A 3 (2015) 19027–19032.
[88] L.L. Feng, G. Yu, Y. Wu, G.D. Li, H. Li, Y. Sun, T. Asefa, W. Chen, X. Zou, J. Am. Chem. Soc. (2015).
[89] Z. Jian, W. Luo, X. Ji, J. Am. Chem. Soc. 137 (2015) 11566–11569.
[90] A.C. Luntz, B.D. McCloskey, Chem. Rev. 114 (2014) 11721–11750.
[91] S. Zhang, Z. Wen, K. Rui, C. Shen, Y. Lu, J. Yang, J. Mater. Chem. A 3 (2015) 2568–2571.
[92] W. Zhang, J. Zhu, H. Ang, Y. Zeng, N. Xiao, Y. Gao, W. Liu, H.H. Hng, Q. Yan, Nanoscale 5 (2013) 9651–9658.
[93] N. Zhao, C. Li, X. Guo, Phys. Chem. Chem. Phys. 16 (2014) 15646–15652.
[94] S. Liu, Z. Wang, C. Yu, Z. Zhao, X. Fan, Z. Ling, J. Qiu, J. Mater. Chem. A 1 (2013) 12033–12037.
[95] H. Nie, C. Xu, W. Zhou, B. Wu, X. Li, T. Liu, H. Zhang, ACS Appl. Mater. Interfaces 8 (2016) 1937–1942.
[96] W.-J. Kwak, Z. Chen, C.S. Yoon, J.-K. Lee, K. Amine, Y.-K. Sun, Nano Energy 12 (2015) 123–130.
[97] B. Sun, S. Chen, H. Liu, G. Wang, Adv. Funct. Mater. 25 (2015) 4436–4444.
[98] Z. Zhang, J. Bao, C. He, Y. Chen, J. Wei, Z. Zhou, Adv. Funct. Mater. 24 (2014) 6826–6833.
[99] M.M. Ottakam Thotiyl, S.A. Freunberger, Z. Peng, P.G. Bruce, J. Am. Chem. Soc. 135 (2013) 494–500.
[100] M.M.O. Thotiyl, S.A. Freunberger, Z. Peng, Y. Chen, Z. Liu, P.G. Bruce, Nat. Mater. 12 (2013) 1050–1056.
[101] D. Kundu, R. Black, B. Adams, K. Harrison, K.R. Zavadil, L.F. Nazar, J. Phys. Chem. Lett. 6 (2015) 2252–2258.
[102] C. Xu, B.M. Gallant, P.U. Wunderlich, T. Lohmann, J.R. Greer, ACS Nano 9 (2015) 5876–5883.
[103] K.G. Gallagher, S. Goebel, T. Greszler, M. Mathias, W. Oelerich, D. Eroglu, V. Srinivasan, Energy Environ. Sci. 7 (2014) 1555–1563.
[104] K. Takechi, T. Shiga, T. Asaoka, Chem. Commun. 47 (2011) 3463.
[105] S.R. Gowda, A. Brunet, G.M. Wallraff, B.D. McCloskey, J. Phys. Chem. Lett. 4 (2013) 276–279.
[106] H.-K. Lim, H.-D. Lim, K.-Y. Park, D.-H. Seo, H. Gwon, J. Hong, W.A. Goddard, H. Kim, K. Kang, J. Am. Chem. Soc. 135 (2013) 9733–9742.
[107] Y. Liu, R. Wang, Y. Lyu, H. Li, L. Chen, Energy Environ. Sci. 7 (2014) 677–681.
[108] S. Xu, S.K. Das, L.A. Archer, RSC Adv. 3 (2013) 6656.
[109] Z. Zhang, Q. Zhang, Y. Chen, J. Bao, X. Zhou, Z.J. Xie, J.P. Wei, Z. Zhou, Angew. Chem. Int. Ed. 54 (2015) 6550–6553.
[110] X. Zhang, Q. Zhang, Z. Zhang, Y. Chen, Z. Xie, J. Wei, Z. Zhou, Chem. Commun. 51 (2015) 14636–14639.
[111] S. Meini, M. Piana, N. Tsiouvaras, A. Garsuch, H.A. Gasteiger, Electrochem. Solid-State Lett. 15 (2012) A45–A48.
[112] N.B. Aetukuri, B.D. McCloskey, J.M. García, L.E. Krupp, V. Viswanathan, A.C. Luntz, Nat. Chem. 7 (2014) 50–56.
[113] F. Li, S. Wu, D. Li, T. Zhang, P. He, A. Yamada, H. Zhou, Nat. Commun. 6 (2015) 7843.
[114] C. Xia, R. Black, R. Fernandes, B. Adams, L.F. Nazar, Nat. Chem. 7 (2015) 496–501.
[115] T. Liu, M. Leskes, W. Yu, A.J. Moore, L. Zhou, P.M. Bayley, G. Kim, C.P. Grey, Science 350 (2015) 530–533.